Int. J. Electrochem. Sci., 10 **(2015)** 6558 - 6571

International Journal of
ELECTROCHEMICAL
SCIENCE
www.electrochemsci.org

Polypyrrole Nanotubes Decorated with Gold Particles Applied for Construction of Enzymatic Bioanodes and Biocathodes

Markéta Ilčíková[1], *Jaroslav Filip*[2], *Miroslav Mrlík*[1], *Tomáš Plachý*[3], *Ján Tkáč*[2,*], *Peter Kasák*[1,*]

[1] Center for Advanced Materials, Qatar University, P.O.Box 2713, Doha, Qatar.
[2] Department of Glycobiotechnology, Institute of Chemistry, Center for Glycomics, Slovak Academy of Sciences, Dubravska cesta 9, Bratislava 845 38, Slovak Republic
[3] Centre of Polymer Systems, University Institute, Tomas Bata University in Zlin, Nad Ovcirnou 3685, 760 01, Zlín, Czech Republic
[*]E-mail: Peter.Kasak@qu.edu.qa, Jan.Tkac@savba.sk

Received: 9 April 2015 / *Accepted:* 8 June 2015 / *Published:* 24 June 2015

The novel composites of gold nanoparticles and polypyrrole nanotubes (Au_x@PNT) were prepared and used as a platform for fabrication of bioelectrode interfaces. Changing the conditions of composite preparation caused variations in a gold architecture, electrical conductivity and a biocompatibility. These features could be easily adjusted by setting up a proper fabrication protocol. The Au_x@PNT-chitosan matrix was utilized for fabrication of bioelectrode interfaces with physisorbed oxidoreductases. Biocatalytic activity of such physisorbed fructose dehydrogenase (FDH), laccase (Lac) and bilirubin oxidase (BOD) was investigated with biocatalytic current density up to j = 2.45 mA cm^{-2} obtained for a bioanode based on direct electron transfer of FDH. Performance of biocathodes with immobilized Lac and BOD showed current density up to 232 µA cm^{-2} in presence of a redox mediator.

Keywords: polypyrrole nanotubes, bilirubin oxidase, laccase, fructose dehydrogenase, biofuel cells, gold nanoparticles

1. INTRODUCTION

Polypyrrole (PPy) as a conducting polymer exhibits high electrical conductivity, excellent environmental and thermal stability, good antibacterial properties and sufficient biocompatibility [1,2]. Such properties are promising for many bioapplications [1]. Moreover the one-dimensional forms of nanomaterials such as nanorods, nanofibers or nanotubes exhibit better charge transport properties compared to globular forms. Additionally, large surface area of the nanoscale objects is beneficiary in

many applications especially for development of chemical and biological sensors or for construction of electrochemical and biofuel cells [1].

Composites of noble metals and conductive polymers can be prepared by a simple mixing of noble metal precursor and already synthesized conducting polymer [3-5]. *In-situ* reduction of metal from precursor provides stronger interaction between the components and thus enhanced performance can be reached [6]. Various approaches for preparation Au@PPy composites by *in-situ* oxidation of monomer pyrrole with metal precursor have been reported. *In situ* preparation of such composites has been realised in numerous alternatives including a direct reaction of both components in aqueous solution [7, 8] a procedure requiring additional surfactants [9,10], block copolymers [11,12] or capping agents [13] in order to control the composite structures. The reduction of gold from precursor can occur by already mentioned direct reaction with PPy [14]. This facile approach has attracted our attention since composites with various morphologies and different amount of gold particles can be prepared and properties of the composites can be finely tuned by choosing the reducing agent and reaction conditions.

The utilization of Au in PPy composite was found to have beneficial effect on the electrochemical activity of the electrodes exhibiting enhanced electron transfer [15,16] applied for construction of sensors [17] biosensor interfaces [18], but also for enhanced loading of biomolecules [15].

Besides above mentioned applications, there are numerous examples of an efficient immobilization of oxidoreductases in different PPy structures and matrices achieving detectable electrocatalysis without any electron shuttle involved in a system. Such direct (non-mediated) electron transfer [19] was observed for different oxidoreductases [20,21], including fructose dehydrogenase (FDH) [22-24]. Due to the good electron conductivity, high surface area and biocompatibility, PPy-modified interfaces could be used for fabrication of electrochemical biosensors or anodes of biofuel cells (BFCs).

Other oxidoreductases known to exhibit very fast direct electron transfer (DET) with diverse carbonaceous and metallic nanostructures are “multi copper oxidases” (MCOs) [19,25]. Laccase from *Trametes versicolor* (Lac) and bilirubin oxidase (BOD), belonging to this family of enzymes, accepts electrons *via* its cuprous active site (the “T1” site) and passes them to a second active site where a molecule of dioxygen is bound and consequently reduced to water [21,26]. Due to high rate of this reaction, both enzymes are very broadly employed in fabrication of enzymatic biocathodes applicable mostly in fabrication of BFCs. To achieve DET between the T1 site and the electrode, the enzymes must be oriented properly on the surface what is hard to achieve on surfaces with a positive electrical charge, including PPy [27]. In such cases, bioelectrocatalytic properties of enzymes can be evaluated by employment of soluble electron mediators.

In this study process for preparation Au_x@PNT composites is described with characterization of composites based on reaction condition. Moreover, adopting recently developed methods of BOD adsorption on carbon nanotubes and carbon black particles dispersed in chitosan [28], FDH, BOD and Lac were immobilized on the synthesized PPy nanotubes with gold structure (Au_x@PNT) mixed with chitosan (CHI) forming an Au_x@PNT-CHI interface. Such prepared bioanodes and biocathodes were characterized from a biocatalytic point of view in presence of fructose and oxygen, respectively.

2. EXPERIMENTAL PART

2.1 Materials

Pyrrole (PPy, Riedel-de Haen AG, Germany) was freshly distilled before use. Methyl orange (BDH, England), iron (III) chloride hexahydrate (Breckland Scientific Supplies, UK), sodium borohydride ($NaBH_4$), ascorbic acid (AA), chloroauric acid ($HAuCl_4.3H_2O$), acetone, ethanol (Aldrich, USA) were used as received. Chitosan (CHI, MW = 50–190 kDa), 2,2'-azino-bis(3-ethylbenzothiazoline-6-sulphonic acid (ABTS), bilirubin oxidase from *Myrothecium verrucaria* (BOD) and laccase from *Trametes versicolor* (Lac) were obtained from Sigma-Aldrich (St. Luis, USA). Fructose dehydrogenase from *Gluconobacter oxydans* (FDH) was obtained from Sorachim (Lausanne, Switzerland). Ultrapure water (DW) was obtained by Merck Millipore U.S.A water purification system.

2.2 Synthesis

2.2.1. Polypyrrole nanotubes (PNT)

The synthesis of PNT was performed according to Skodova et al. [5]. The freshly distilled monomer pyrrole (1 mL, 14 mmol) was added to 278 mL of 2.5 mM aqueous solution of methyl orange (0.2348 g, 0.7 mmol). Iron (III) chloride (3.9 g, 14 mmol) was dissolved in 33 mL DW and dropwise added to a reaction mixture within 2 h. The reaction mixture was additionally stirred for 22 h. The particles were filtered, washed with water and finally with ethanol. To completely remove methyl orange, the particles were purified by Soxhlet extraction with acetone until washing solvent became colourless.

2.2.2. Synthesis of Au_x@PNT

Table 1. The reaction conditions for preparation of Au_x@PNT composites

No.	Sample name	Reaction time (days)	Au (III) precursor concentration	Reducing Agent, temperature
1	PNT	-	-	without RA, 20 °C
2	Au_1@PNT	1	0.15 mmol	without RA,20 °C
3	Au_2@PNT	1	0.15 mmol	AA, 20 °C
4	Au_3@PNT	3	0.15 mmol	AA, 20 °C
5	Au_4@PNT	1	1.5 mmol	AA, 20 °C
6	Au_5@PNT	3	1.5 mmol	AA, 20 °C
7	Au_6@PNT	1	1.5 mmol	$NaBH_4$, 20 °C
8	Au_7@PNT	3	1.5 mmol	$NaBH_4$, 20 °C
9	Au_8@PNT	3	1.5 mmol	without RA, 30 °C
10	Au_9@PNT	3	1.5 mmol	without RA, 80 °C

The general procedure for the Au_x@PNT composites preparation is described in the following text while the detailed reaction conditions are summarized in Table 1.

PNT (0.025 g) was dispersed in 8 mL of DW and sonicated shortly with an ultrasonic probe (30 s, 0.4 cycle, 20% amplitude). $HAuCl_4.3H_20$ (0.06 g, 0.15 mmol) was dissolved in DW and added to a reaction mixture followed by addition of 2.5 mL of 0.06 M aqueous solution of a reducing agent (AA or $NaBH_4$). The reaction flask was immersed into an oil bath heated to 30 °C and stirred for specified time. Au_x@PNTs were purified *via* washing and centrifugation (3,000 rpm, 10 min) steps with 24 mL DW (5x) and once with ethanol. The particles were dried at room temperature (RT) overnight and at 60 °C in *vacuum*.

2.3 Bioelectrodes

The Au_x@PNT composites were dispersed in a chitosan solution (0.1% in 0.3% acetic acid) by an ultrasound treatment (1 h). The obtained dispersions (Au_x@PNT@CHI) were drop-casted on surfaces of glassy carbon electrodes (GCE, d=3 mm; BASi, USA) and left to dry under a nitrogen stream, at RT. These modified electrodes (GCE/Au_x@PNT@CHI) were either tested using cyclic voltammetry (CV) or incubated with FDH (3 U μl^{-1}; 5 µl, in 100 mM acetate buffer pH 5), BOD (0.025 U μl^{-1}; 10 µl, in 100 mM phosphate buffer pH 7) or Lac solution (1 U μl^{-1}; 10 µl, in 100 mM acetate buffer pH 5) overnight, capped by an Eppendorf tube to prevent evaporation of the enzyme solution.

2.4 Methods

Transmission electron microscopy (TEM Phillips CM12) was used to confirm the tube-like character of prepared PPy structures. The surface composition was determined by scanning electron microscopy (SEM, FEI Quanta 200) equipped with an energy dispersive X-ray spectroscopy (EDS microanalysis system; FEI, USA). The amount of gold beads was determined by a thermogravimetric analysis (TGA, Mettler Toledo TGA/SDTA 851E) under air flow conditions. The conductivity was measured by a four point van der Pauw method at ambient temperature (Keithley 6517b, USA) on pressed pellets with diameter of 13 mm and thickness 0.2 – 0.3 mm.

Electrochemical measurements were performed using potentiostat Multi Autolab Cabinet (EcoChemie, Utrecht, The Netherlands). Three-electrode connection was used with a modified GCE used as a working electrode and Pt disc (d=3 mm; BASi, USA) and Ag|AgCl|3M KCl (BASi, USA) applied as counter and reference ones, respectively.

3. RESULTS AND DISCUSSION

3.1. Morphology of PNT

The tube-like high aspect ratio structures were obtained due to presence of a structure-guiding agent, methyl orange [5,29]. The PNT contains counter ion after preparation, exhibiting high electrical

conductivity (~ 35.7 S cm^{-1}) [29]. The structure of PNT was confirmed by TEM. In Fig. 1 there are shown one-dimensional high aspect ratio structures with diameter varying between 60-120 nm.

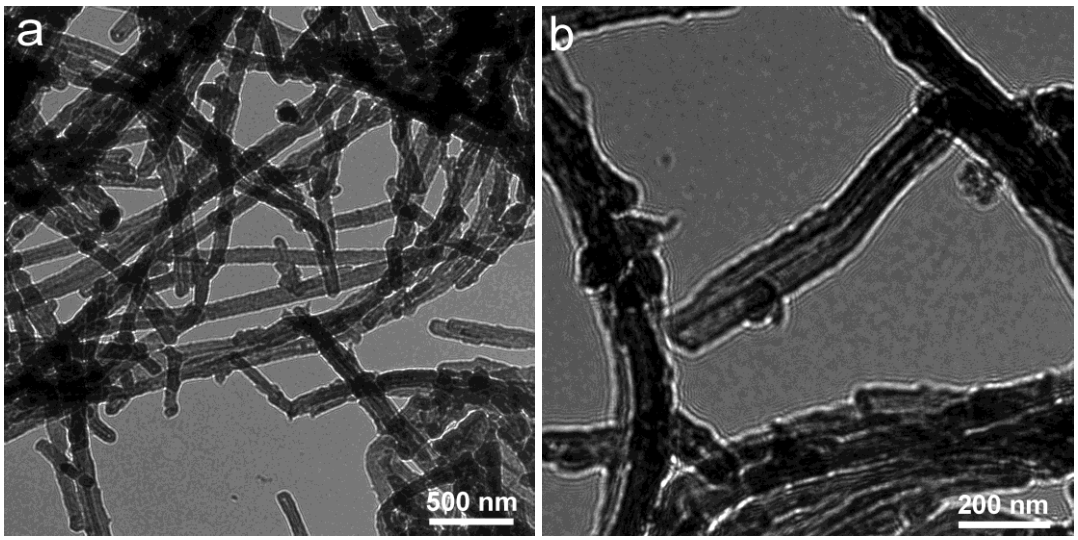

Figure 1. a) TEM images of PNT; b) the detail of PNT with obvious tube-like character.

3.2. Synthesis and morphology of Au_x@PNT

Table 2. Characteristics of prepared Au_x@PNT

No.	Sample Name	Particle size[a]/morphology	Electrical conductivity[b] σ±Δσ (S cm^{-1})	Au content[c] (%)
1	PNT	-	35.7±1.2	0
2	Au_1@PNT	394 ±43 nm/ CNP	15.1±0.9	16
3	Au_2@PNT	680 ± 50 nm /CNP	3.26± 0.06	15
4	Au_3@PNT	790 ± 120 nm/CNP	1.63±0.01	17
5	Au_4@PNT	200 ± 26 nm/CNP	14.5± 0.1	53
6	Au_5@PNT	1080 ± 90 nm /CNP	0.24±0.01	47
7	Au_6@PNT	68 ± 11 nm/NP	28.4± 0.5	57
8	Au_7@PNT	39 ± 15 nm/NP	75.0 ±1.7	61
9	Au_8@PNT	NA	0.507±0.004	34
10	Au_9@PNT	NA	0.362±0.001	34

[a] estimated from SEM images, NA-not analysed

[b] determined by four point method according to van der Pauw

[c] determined by thermogravimetric analysis

The reaction time, $HAuCl_4$ amount and type of a reducing agent were varied during the synthesis of Au_x@PNT composites with details about the reaction conditions listed in Table 1. Three reduction agents were used, i.e. only PNT, AA as a mild reducing agent and $NaBH_4$ as a strong reducing agent. It was observed that Au(III) was reduced to Au(0) nanoparticles in the presence of

PNT alone as well as upon a treatment of a reducing agent, i.e. AA or $NaBH_4$. The effect of a reducing agent and a reaction time on morphology of the synthesized gold particles was investigated using SEM EDS analysis. Two morphological types were observed, the individual nanoparticles (NP) and clusters of nanoparticles (CNP) arranged into architectures similar to those observed by Li et al. [30]. The gold content of the Au_x@PNT was estimated from a thermogravimetric analysis and electrical conductivity measurements were performed by a four-point method according to van der Pauw on compressed pellets. The results are shown in Table 2.

PNT was applied as a reagent to reduce Au(III) and create clusters with size of 394±43 nm (Fig. 2). Mechanism of reduction of Au by PNT can be explained by partial transformation of PNT from emeraldine to pernigraniline state. The proposed mechanism for reduction of Au(III) to Au(0) was similarly described previously [14] and similar observation was reported to reduce silver by PPy from $AgNO_3$ [5].

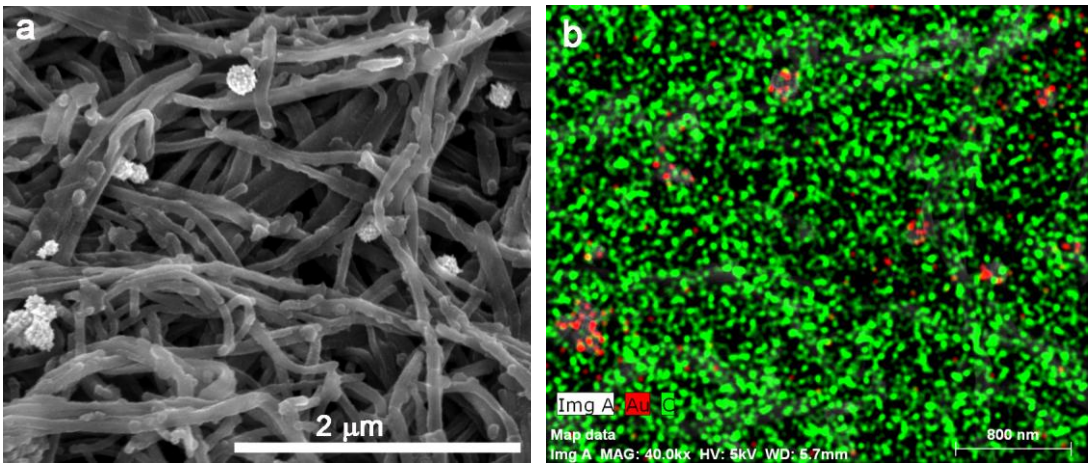

Figure 2. a) SEM image of Au_1@PNT, b) SEM EDS analysis of Au_1@PNT with Au visualized in red and C in green.

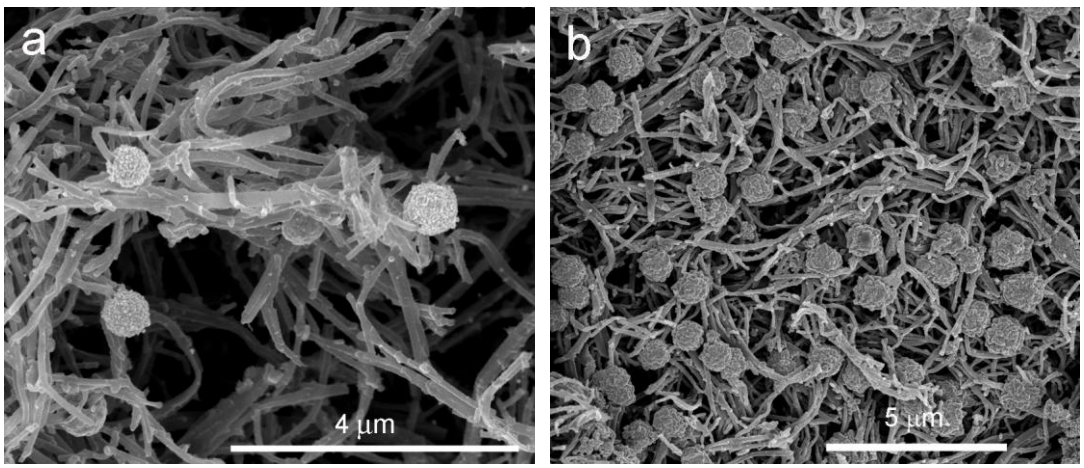

Figure 3. SEM images of after formation of Au clusters in presence of AA produced a) in one day (Au_2@PNT) and b) in three days (Au_5@PNT).

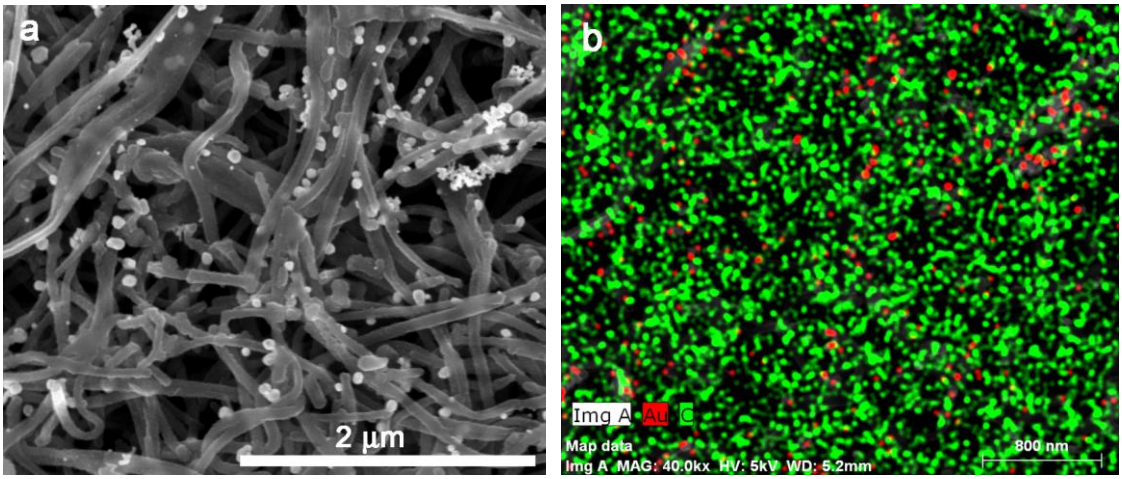

Figure 4. a) SEM image of Au_7@PNT, b) SEM EDS analysis of Au_7@PNT with Au visualized in red and C in green.

Production of gold nanoparticles with a mild reducing agent AA resulted in formation of 680 ± 50 nm clusters (Au_2@PNT, Fig. 3a). Upon prolongation of a reaction time to three days, with a ten-fold increased initial concentration of Au(III), formation of larger 1080 ± 90 nm clusters was observed (Au_5@PNT, Fig. 3b). On the other hand, application of a stronger reducing agent, $NaBH_4$, resulted in formation of individual nano-sized (68 ± 11 nm) particles (Au_6@PNT). The prolonged reaction time did not lead to formation of Au particle clusters, instead, smaller nanoparticles were observed (39 ± 15 nm, Au_7@PNT, Fig. 4).

The difference in the size and morphology of Au objects is most likely related to efficiency of a reducing agent applied. Au is reduced from Au(III) to Au(0) in two consecutive steps. First, Au(III) is reduced to Au(I) state, and then to Au(0). While the first step, i.e. reduction of Au(III) to Au(I) state, is related to nuclei formation, the following reduction to Au(0) is responsible for nanoparticle formation and growth [31]. Apparently the second reduction step is responsible for formation of the clusters. Since AA is a weaker reducing agent compared to $NaBH_4$, longer time needed for nanoparticle formation in presence of AA resulted in development of Au microstructures over time. These observations are consistent with results obtained by Li et. Al [30], who reported formation of raspberry-like gold microspheres from an Au(I) precursor.

The small amount of Au present in the Au_x@PNT composite resulted in a decrease of an electrical conductivity (σ) compared to PNT regardless of a reducing agent and reaction time applied (protocols No. 2, 3, 4). In these cases comparable amount of gold (~ 15 %) was present in the composite formed.

The moderate decrease of σ in the composites consisted of Ag and PPy (Ag@PPy) was reported by Skodova et al.[5]. While PPy nanotubes in form of salt exhibited σ of 35.7 S cm^{-1}, the reduction of Ag(I) salt to nanoparticles resulted in decrease of σ to a value of 0.028 S cm^{-1} in Ag@PPy [5]. Similar effect of metallic nanoparticles on σ was reported by Bober et al. in a composite based on silver and polyaniline (Ag@PANI) [32] and a composite containing Ag and a copolymer poly[aniline-co-(p-phenylenediamine)] [33]. The charge transport mechanism in such systems was recognized as a variable range electron hopping [34], where the charge carrier have to overcome by hopping an energy

barrier to provide the current. The presence of metallic particles introduces a certain inhomogeneity into the system, hence the hopping distance increases that reflects in decreased σ. The presence of metallic particles hinders the charge transport up to certain concentration, close to 60 wt% [33].

All nanohybrids prepared by AA treatment exhibited substantially lower conductivity compared to PNT, nevertheless, this decrease was smaller when 10-fold higher initial concentration of Au precursor was used (2-fold decrease for 1.15 *vs*. 10-fold decrease for 0.115 mmol of $HAuCl_4$; protocols No. 3 and 5). Interestingly, upon prolongation of reaction time the observed pattern was reversed, i.e. higher amount of gold precursor caused more rapid conductivity decrease (protocols No. 4 and 6). As was observed in SEM EDS analysis, the micro-sized Au clusters are formed in the presence of AA with their size growing in time. On the other hand the nanoparticles formed in the presence of $NaBH_4$ after 3 days exhibited an increased electrical conductivity (protocol No. 8). For comparison, the nanoparticles prepared without any reducing agent reduced smaller amount of Au(III) compared to those using $NaBH_4$ or AA and their irregular shape led to electrical conductivity decrease (protocol No. 9). The effect of temperature up to 80 degree was investigated as well, however no impact on gold amount and electrical conductivity was found (protocol No.10).

The electrical conductivity of Au_x@PNT was found to be more sensitive to size of the formed clusters than to Au amount. The correlation of σ with particles size is shown in Figure 5. As was mentioned above, the system with increasing of size of Au architecture hindered the charge transport, resulting in dramatic drop of σ.

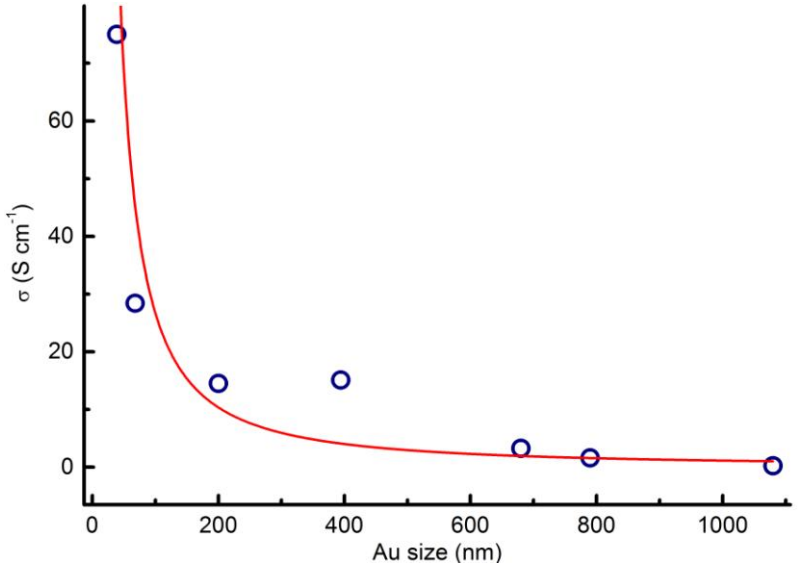

Figure 5. Dependence of electrical conductivity on the size of Au clusters.

3.3. Biocompatibility of the Au_x@PNT

CVs of the modified electrodes revealed that all composites are electrochemically active as deduced from capacitance currents determined on all electrodes (e.g. see Fig. 6). Nevertheless, it was found that capacitance currents varied strongly among composites tested indicating different amount of

electrochemically active Au_x@PNT on the electrodes. Due to the fact that all dispersions were prepared using the same initial concentration of nanomaterials, it is reasonable to conclude that the stability of the formed Au@PNT@CHI film depends mainly on a composition of the Au@PNT component. It should be noted that this parameter, i.e. stability of the composite film, was not optimized.

3.4. FDH-based anodes

After deposition of FDH on modified GCEs, the obtained bioelectrodes were tested electrochemically in a buffer containing 100 mM D-fructose. In order to achieve unbiased biocatalytic currents, voltammograms obtained on the electrodes measured in a buffer without the enzyme's substrate were subtracted from the curves obtained in the presence of D-fructose. From such background-corrected CVs, maximum biocatalytic currents I_{CAT} were read typically between 300 and 400 mV (Fig. 6).

From all tested samples, the highest values of I_{CAT} were provided by the electrodes coated with the PNT-CHI dispersion without gold particles (j = 2.45 ± 0.39 mA cm^{-2}), followed by the bioanodes GCE/Au_3@ PNT@CHI/FDH (j = 1.74 ± 0.46 mA cm^{-2}) and GCE/Au_7@PNT@CHI/FDH (j = 1.6 mA cm^{-2}). It should be noted that all measurements were performed in quiescent solution and without any mediator.

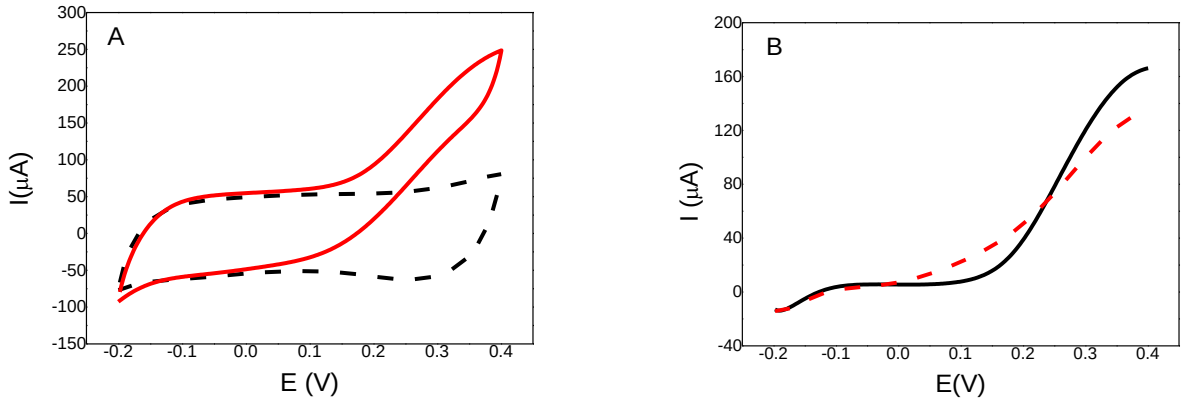

Figure 6. (**A**) Typical CVs of the GCE/Au_3@PNT@CHI/FDH electrodes in absence (black) and presence (red) of 100 mM fructose. (**B**) – biocatalytic waves of GCE/ Au_3@PNT@CHI/FDH electrode shown in panel A (black) compared to a biocatalytic wave of GCE/PNT@CHI/FDH (red). All measurements performed in 100 mM acetate buffer pH 5 at a scan rate of 50 mV s^{-1}.

Electrical conductivity seems to partially correlate with the value of the biocatalytic activity of the prepared bioanodes as can be seen in Fig. 7, where the obtained values of current densities j are plotted against the conductivity of the composites. It was revealed that Au_1@PNT and Au_4@PNT exhibited the same level of σ and even their biocatalytic current densities were quite similar, i.e. 0.75±0.06 mA cm^{-2} (GCE/Au_1@PNT-CHI/FDH) and 1.1 mA cm^{-2} (GCE/Au_4@PNT-CHI/FDH). A

good linear correlation σ *vs. j* was valid also for GCE/PNT-CHI/FDH and GCE/Au_5@PNT-CHI/FDH bioelectrodes as can be seen from a linear fit presented in Fig. 7 (solid black line). Besides showing an excellent linearity between conductance and biocatalytic current density (R^2 = 0.953), the graph also unveiled that the GCE/Au_3@PNT-CHI/FDH biocathode did not fit into this pattern, it provided a current density close to the level of biocathodes prepared from unmodified PNTs even though the composite exhibited very low electric conductivity. This behaviour can be explained by very large surface area of gold CNP allowing adsorption of substantially larger amount of FDH compared to composites with smaller gold nanoparticles. Apparently, conductivity of the Au_3@PNT composite is, although low, enough to secure very high catalytic current. This is obviously not a case of the Au_5@PNT composite where more gold CNP could be detected (see Fig. 3b). Here, the conductivity decreased below the threshold necessary for a fast transport of electric charge from the enzyme molecules towards the GCE surface. This is most probably why only a current density of 0.27±0.012 mA cm^{-2} was obtained with GCE/Au_5@PNT-CHI/FDH bioanode.

Au_7@PNT is another composite which did not fit in the linear dependence σ vs. *j*. Here, unlike for Au_3@PNT, the bottleneck of a biocatalytic current generation is most probably in a small active surface area of the grown gold nanoparticles. It is supported by SEM images (Fig. 4) as well as by a conductivity of Au_7@PNT reaching values even higher than that for unmodified PNTs. This would suggest that gold nanoparticles are that abundant that they can secure long-range electron transfer instead of or, more likely, in parallel with the electron transfer alongside the single PNTs.

Under the given conditions and preparation protocols, it can be said that the Au3@PNT3 composite is, among all the tested Au_x@PNT nanomaterials, the most convenient for adsorption of FDH because it is conductive enough and at the same time it can bear very high amount of electrocatalytically active FDH molecules.

It should be noted that the obtained current density for the GCE/ Au_3@PNT-CHI/FDH electrode is comparable to current density obtained on interfaces employing FDH adsorbed on carbon cryogel [35], carbon black [36] and gold nanoparticles [37]. It cannot compete, however, with systems where enzymes and nanotubes are aligned more tightly [20], but substantial increase of current densities can be achieved for example by employment of highly porous electrode substrate instead of a planar GCE disc electrode [37]. Swann et al. [23] has calculated a maximum current density as high as 11 mA cm^{-2} can be theoretically obtained using FDH entrapped in polypyrrole matrix, but their measurements revealed an efficiency of only 2.4% and a real measured maximum current density of 5 μA cm^{-2}. Low diffusion of fructose to the enzyme was recognized as a major cause of low efficiency [23] suggesting that PPy nanotubes provide more space for effective mass transport compared to more easily fabricated PPy matrices. On the other side, current density of 1.2 mA cm^{-2} was reported when FDH was entrapped into polypyrrole matrix with co-polymerized mediator [38]. Also, it is important to note that even though unmodified PNTs-based electrodes provided slightly higher current density than the best-performing Au@PNT composite, gold particles were important for improving stability of the electrode-coating films due to the efficient coupling between amino groups of chitosan and gold surface. The stability was confirmed even visually – after a mild rinsing of modified GCE, PNT-CHI films were more prone to be partially washed out from the surface than the samples containing gold particles.

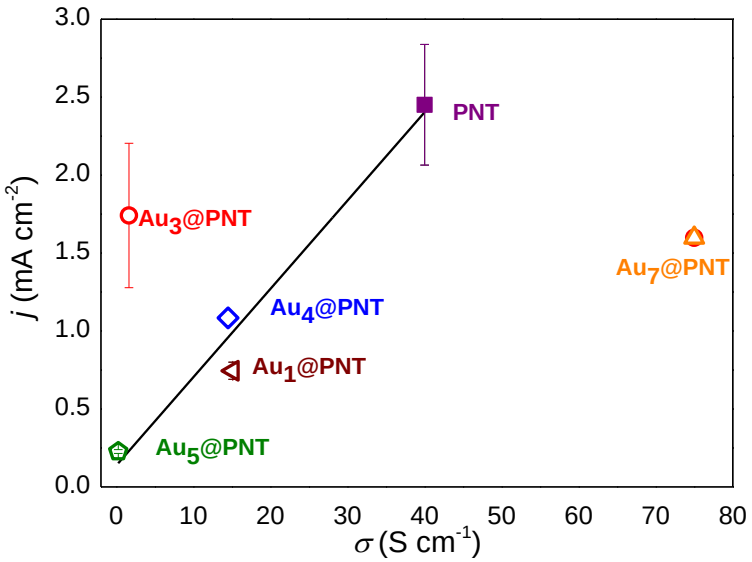

Figure 7. Mean current densities of tested GCE/Au_x@PNT-CHI/FDH electrodes, including standard deviations, plotted against electrical conductivity of individual Au_x@PNT composites. Linear dependence of current densities of bioanodes prepared from PNT, Au_1@PNT, Au_4@PNT and Au_5@PNT composites is shown (solid black line).

3.5. Biocathodes

As expected [27], none of MCOs immobilized on selected modified electrodes exhibited significant biocatalytic current in presence of oxygen, most probably due to high abundance of amino-groups of PNTs causing improper orientation of enzymes and thus disabling DET between MCO and PNTs. Nevertheless, presence of active BOD was confirmed by performing CVs in a phosphate buffer containing electron mediator ABTS. These measurements revealed a value of $j = 232 \pm 64$ μA cm^{-2} for BOD adsorbed on GCE/PNT-CHI electrode while lower values of 86 and 82 ± 4 μA cm^{-2} were observed on the Au_1@PNT-CHI and Au_3@PNT-CHI-based biocathodes, respectively (data not shown). In similarity with experiments involving FDH, the Au_3@PNT-CHI composite appeared to be rather improper platform for the enzyme adsorption, or, more precisely, there was probably low surface activity securing regeneration of ABTS. CVs of Au_5@PNT-CHI-based biocathode revealed less than a halve value of *j* compared to the Au_3@PNT-CHI biocathode (data not shown).

Lac had also provided an ABTS-mediated biocatalytic response on the GCE/ Au_4@PNT-CHI and GCE/PNT-CHI electrodes. While with the former one a biocatalytic current density $j = 94 \pm 24$ μA cm^{-2} (less than 1 μA cm^{-2} without ABTS) was observed, a value of $j = 34 \pm 9$ μA cm^{-2} (3.5 μA cm^{-2} without ABTS) was measured on the PNT-CHI/Lac electrode (Fig. 8). All *I* values were read at 200 mV to avoid interferences from faradaic processes others than enzymatically catalysed oxygen reduction. It should be also noted that these values were obtained with biocathodes prepared from 1 mg ml^{-1} PNT and Au_4@PNT-CHI dispersions since application of a higher concentration (i.e. 5 mg ml^{-1}) produced rather inconsistent data.

It can be concluded that gold particles coating the conductive nanotubes were helpful in adsorption of Lac, contrary to BOD. It is quite consistent with results obtained for example by

Ulyanova et al. [39], who revealed different nature of electrostatic interaction of these two enzymes with interfaces.

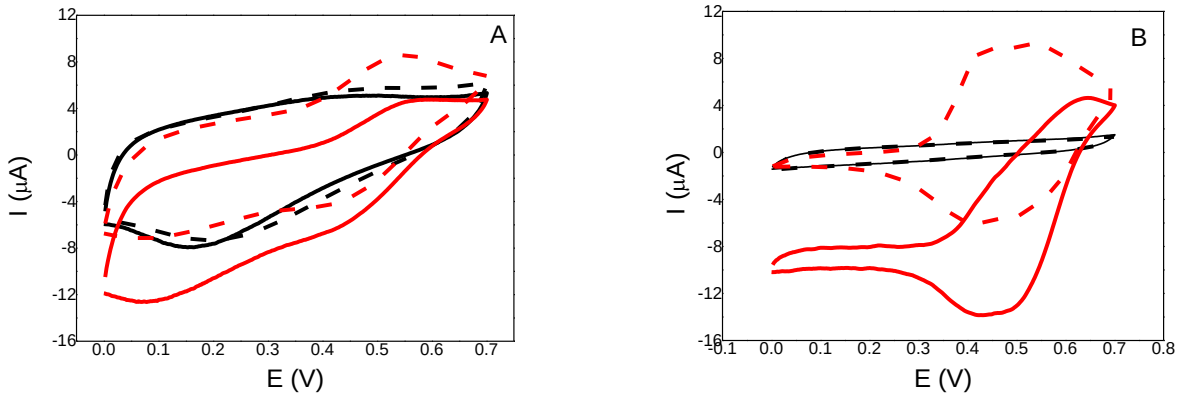

Figure 8. CVs of GCE/PNT-CHI/Lac (panel A) and GCE/Au_4@PNT-CHI/Lac (panel B) biocathodes performed in 100 mM acetate buffer pH 5 (all black curves) and the same buffer containing 2 mM ABTS (all red curves). Electrolytes were either deaerated using N_2 (all dashed lines) or air-bubbled (all solid lines). Step potential 10 mV s^{-1}.

4. CONCLUSIONS

PNT composites decorated with gold particles were synthesized and size, morphology and amount of gold nano- or micro- particles can be adjusted by reducing agent and time preparation, thus composites with varied electrical conductivity could be prepared.

Three oxidoreductases i.e. fructose dehydrogenase, bilirubin oxidase and laccase were physisorbed from their solutions on the prepared nanostructured electrode interfaces from dispersions of Au_x@PNT in chitosan matrix and their catalytic activity was tested electrochemically.

It was found that FDH binds strongly and effectively to PNT dispersed in chitosan and large biocatalytic currents (2.45±0.39 mA cm^{-2}) are detected at this electrode. Au_3@PNT provided the interface most suitable for FDH adsorption, achieving biocatalytic current density of 1.74±0.46 mA cm^{-2} without mediator. Amount of FDH adsorbed on gold CNP have been shown to play more important role than conductivity until very low values of σ have been achieved.

In case of adsorbed bilirubin oxidase and laccase substantial biocatalytic current response were provided only in a presence of electron mediator ABTS. Application of BOD resulted in larger biocatalytic currents on more conductive GCE/PNT-CHI/BOD electrodes (j = 232±64 μA cm^{-2}) while the BOD adsorbed on interfaces containing gold particles provided only about a one third of this value.

On the other side, experiments with laccase revealed that this enzyme provided larger mediated catalytic currents when immobilized on Au@PNT-CHI interface than on a PNT-CHI surface. Under the given conditions (i.e. mainly lower pH than used for probing of BOD-based biocathodes), either

electrochemical regeneration of mediator ABTS or an amount of active Lac adsorbed on the surface is promoted by a presence of gold nanoparticles.

ACKNOWLEDGEMENTS
We thank to Central Laboratory Unit, Qatar University, for carrying out SEM and TEM analysis. This publication was made possible by NPRP grant # 6-381-1-078 from the Qatar National Research Fund (a member of Qatar Foundation). The statements made herein are solely the responsibility of the authors.

References

1. A. Ramanavičius, A. Ramanavičienė and A. Malinauskas, *Electrochim. Acta* 51 (2006) 6025.
2. E. Nazarzadeh Zare, M. Mansour Lakouraj and M. Mohseni, *Synth. Met.* 187 (2014) 9.
3. D. M. Chao, L. L. Cui, J. F. Zhang, X. C. Liu, Y. X. Li, W. J. Zhang and C. Wang, *Synth. Met.* 159 (2009) 537.
4. F. N. Crespilho, R. M. Iost, S. A. Travain, O. N. Oliveira and V. Zucolotto, *Biosens. Bioelectron.* 24 (2009) 3073.
5. J. Skodova, D. Kopecky, M. Vrnata, M. Varga, J. Prokes, M. Cieslar, P. Bober and J. Stejskal, *Polymer Chem.* 4 (2013) 3610.
6. P. Gomez-Romero, *Adv. Mater.* 13 (2001) 163.
7. M. C. Henry, C. C. Hsueh, B. P. Timko and M. S. Freund, *J. Electrochem. Soc.* 148 (2001) D155.
8. L. Mikoliunaite, R. Kubiliute, A. Popov, J. Voronovic, S. Sakirzanovas, A. Ramanaviciene and A. Ramanavicius, *Chemija* 25 (2014) 63.
9. Y. Q. Miao, X. H. Wu, J. R. Chen, J. W. Liu and J. X. Qiu, *Gold Bull.* 41 (2008) 336.
10. S. X. Xing, L. H. Tan, M. X. Yang, M. Pan, Y. B. Lv, Q. H. Tang, Y. H. Yang and H. Y. Chen, *J. Mater. Chem.* 19 (2009) 3286.
11. S. T. Selvan, T. Hayakawa, M. Nogami and M. Moller, *J. Phys. Chem. B* 103 (1999) 7441.
12. S. T. Selvan, J. P. Spatz, H. A. Klok and M. Moller, *Adv. Mater.* 10 (1998) 132.
13. J. Zhang, X. H. Liu, S. H. Wu, H. Y. Xu and B. Q. Cao, *Sens. Actuat. B: Chem.* 186 (2013) 695.
14. E. T. Kang, Y. P. Ting and K. L. Tan, *J. Appl. Polym. Sci.* 53 (1994) 1539.
15. T. An, W. Choi, E. Lee, S. J. Cho and G. Lim, *J. Nanosci. Nanotechnol.* 12 (2012) 4975.
16. J. Njagi and S. Andreescu, *Biosens. Bioelectron.* 23 (2007) 168.
17. J. Li, H. Xie and Y. Li, *J. Solid State Electrochem.* 16 (2012) 795.
18. H. Maria, in *Functional Nanoparticles for Bioanalysis, Nanomedicine, and Bioelectronic Devices Volume 1*, American Chemical Society, 2012, vol. 1112, pp. 147.
19. S. Shleev, J. Tkac, A. Christenson, T. Ruzgas, A. I. Yaropolov, J. W. Whittaker and L. Gorton, *Biosens. Bioelectron.* 20 (2005) 2517.
20. J. A. Cracknell, T. P. McNamara, E. D. Lowe and C. F. Blanford, *Dalton Trans.* 40 (2011) 6668.
21. T. Miyake, K. Haneda, S. Yoshino and M. Nishizawa, *Biosens. Bioelectron.* 40 (2013) 45.
22. G. F. Khan, E. Kobatake, H. Shinohara, Y. Ikariyama and M. Aizawa, *Anal. Chem.* 64 (1992) 1254.
23. M. J. Swann, D. Bloor, T. Haruyama and M. Aizawa, *Biosens. Bioelectron.* 12 (1997) 1169.
24. J. Tkac, J. Svitel, I. Vostiar, M. Navratil and P. Gemeiner, *Bioelectrochem.* 76 (2009) 53.
25. J. Filip and J. Tkac, *Electrochim. Acta* 136 (2014) 340.
26. J. Filip, R. Monosik and J. Tkac, *Int. J. Electrochem. Sci.* 9 (2014) 2491.
27. R. J. Lopez, S. Babanova, Y. Ulyanova, S. Singhal and P. Atanassov, *ChemElectroChem* 1 (2014) 241.
28. J. Filip, J. Šefčovičová, P. Gemeiner and J. Tkac, *Electrochim. Acta* 87 (2013) 366.
29. J. Kopecka, D. Kopecky, M. Vrnata, P. Fitl, J. Stejskal, M. Trchova, P. Bober, Z. Moravkova, J.

Prokes and I. Sapurina, *RSC Adv.* 4 (2014) 1551.
30. Z. H. Li, V. Ravaine, S. Ravaine, P. Garrigue and A. Kuhn, *Adv. Funct. Mater.* 17 (2007) 618.
31. M. Luty-Blocho, K. Paclawski, M. Wojnicki and K. Fitzner, *Inorg. Chim. Acta* 395 (2013) 189.
32. P. Bober, J. Stejskal, M. Trchová and J. Prokeš, *Polymer* 52 (2011) 5947.
33. P. Bober, J. Stejskal, M. Trchová, J. Prokeš and I. Sapurina, *Macromolecules* 43 (2010) 10406.
34. R. Moucka, M. Mrlik, M. Ilcikova, Z. Spitalsky, N. Kazantseva, P. Bober and J. Stejskal, *Chem. Pap.* 67 (2013) 1012.
35. S. Tsujimura, A. Nishina, Y. Hamano, K. Kano and S. Shiraishi, *Electrochem. Commun.* 12 (2010) 446.
36. Y. Kamitaka, S. Tsujimura, N. Setoyama, T. Kajino and K. Kano, *Phys. Chem. Chem. Phys.* 9 (2007) 1793.
37. K. Murata, M. Suzuki, K. Kajiya, N. Nakamura and H. Ohno, *Electrochem. Commun.* 11 (2009) 668.
38. A. Begum, E. Kobatake, T. Suzawa, Y. Ikariyama and M. Aizawa, *Anal. Chim. Acta* 280 (1993) 31.
39. Y. Ulyanova, S. Babanova, E. Pinchon, I. Matanovic, S. Singhal and P. Atanassov, *Phys. Chem. Chem. Phys.* 16 (2014) 13367.